Saudi Journal of Ophthalmology (2012) 26, 373–383

Oculoplastic Imaging Update

Orbital masses CT and MRI of common vascular lesions, benign tumors, and malignancies

Sarah N. Khan, MD; Ali R. Sepahdari, MD *

Abstract

A wide variety of space occupying lesions may be encountered in the orbit. CT and MR imaging frequently help confirm the presence of a mass and define its extent. Characteristic imaging features may help distinguish among lesions that have overlapping clinical presentations. This review focuses on some of the common orbital masses. Common vascular lesions that are reviewed include: capillary (infantile) hemangioma, cavernous hemangioma (solitary encapsulated venous-lymphatic malformation), and lymphangioma (venous-lymphatic malformation). Benign tumors that are reviewed include: optic nerve sheath meningioma, schwannoma, and neurofibroma. Malignancies that are reviewed include: lymphoma, metastasis, rhabdomyosarcoma, and optic glioma. Key imaging features that guide radiological diagnosis are discussed and illustrated.

Keywords: Benign orbital masses, Orbital vascular lesions, Malignant orbital masses, Pediatric orbital masses

http://dx.doi.org/10.1016/j.sjopt.2012.08.001

Introduction

A wide variety of processes can produce space-occupying lesions in and around the orbit. These include benign neoplasms, malignant neoplasms, vascular lesions, inflammatory disease, congenital lesions, and infection, among other causes. Imaging can be used to precisely localize a lesion, to help establish a diagnosis or generate a differential diagnosis that guides management, to follow a known lesion for progression, or some combination of these.

The first step in establishing a differential diagnosis is obtaining an accurate clinical history. CT is excellent for confirming the presence of a mass, is well tolerated, can be rapidly obtained at most medical centers, and gives clues to the specific diagnosis. Although MRI can be more difficult to perform, it can reveal additional key imaging features that allow one to more confidently distinguish between similar appearing lesions, and often arrive at a single most likely diagnosis.

Our goal is to review the most commonly encountered lesions to make the reader aware of their typical appearances and presentations, with emphasis on key imaging features that may distinguish among similar lesions.

This review focuses on the most common vascular masses, benign neoplasms, and malignant neoplasms. Due to space constraints, infection[1–3] and inflammatory disease[3–6] are not discussed here. In addition, a number of other vascular lesions and neoplasms are not discussed, including orbital venous varix,[3,7,8] arteriovenous malformation,[3,9] cavernous sinus thrombosis,[3,10] carotid cavernous fistula,[3,7,8] a variety of benign and malignant mesenchymal tumors,[3,11,12] epithelial neoplasms of the lacrimal apparatus,[3,7,13–15] and ocular tumors that secondarily involve the orbit.[3,7] One may also encounter other masses that are not true neoplasms, such as dermolipomas,[3,16,17] dermoid cysts,[3,18–20] and epidermoid cysts.[3,20] For discussion of these lesions, and others, we direct the reader to the referenced sources.

Available online 17 August 2012

Department of Radiological Sciences, David Geffen School of Medicine, University of California Los Angeles, Los Angeles, United States

* Corresponding author. Address: Department of Radiological Sciences, David Geffen School of Medicine, University of California Los Angeles, 757 Westwood Plaza, Suite 1621D, Los Angeles, CA 90095, United States. Tel.: +1 310 267 9785; fax: +1 310 267 3635.
e-mail addresses: ali.sepahdari@gmail.com, asepahdari@mednet.ucla.edu (A.R. Sepahdari).

Peer review under responsibility of Saudi Ophthalmological Society, King Saud University

Production and hosting by Elsevier

Access this article online:
www.saudiophthaljournal.com
www.sciencedirect.com

Vascular lesions

Capillary hemangioma (infantile hemangioma)

Clinicopathologic features

Although the term ''hemangioma'' is sometimes used to describe certain vascular malformations, it more appropriately describes a true neoplasm with vascular channels lined by proliferating endothelial cells.[21] Capillary hemangiomas are the commonest tumors of infancy,[7,22–24] typically appearing as a reddish macule in the first 6 months of life. A proliferative phase occurs up to 10 months, followed by a slow involution phase for up to 10 years.[21,25,26] Though typically sporadic, they may occur as part of a genetic syndrome such as PHACES syndrome.[25]

Imaging findings

Contrast enhanced MRI is the preferred modality for imaging hemangioma, although CT can also be considered if it is not possible to sedate the patient for MRI. The diagnosis is typically well-established clinically, but imaging is indicated to assess the extent of the lesion and mass effect on adjacent structures. With deep lesions, the clinical diagnosis may be challenging. Capillary hemangioma typically shows: (1) lobular contour borders, (2) bright T2 signal with T2 dark septa between lobules, (3) fine internal flow voids, (4) intense, homogeneous enhancement, and (5) preservation of adjacent bone (Fig. 1). Capillary hemangioma can have an atypical appearance without all of these features. Nevertheless, if these features are not all present, then alternative diagnoses should be considered, including rhabdomyosarcoma. DWI may help distinguish these lesions in challenging cases, as rhabdomyosarcoma typically shows lower ADC and brighter DWI signal than hemangioma.[27–29] CT may demonstrate bony orbital expansion or scalloping with rapidly growing lesions. True bone invasion and calcifications are rarely seen.

CT and MR may both demonstrate fat deposition and heterogeneous appearing enhancement, if imaging is performed during the involution phase.[9,23–25]

Differential diagnosis

Rhabdomyosarcoma, vascular malformation, infantile fibromatosis, and infantile fibrosarcoma.

Key features

Bright T2 signal, lobular borders, fine internal flow voids, extraconal location, and intense homogeneous enhancement.

'Cavernous hemangioma' (solitary, encapsulated venous-lymphatic malformation)

Clinicopathologic features

'Cavernous hemangioma' is a term that is widely used to describe a solitary, encapsulated venous-lymphatic malformation, the most common vascular lesion of the orbit.[30] The typical clinical presentation is of mostly painless proptosis (mean 5–6 mm), pain, lid swelling, diplopia, lump, and recurrent obstructed vision. Middle-aged women are the most commonly affected group, and the average duration from symptom onset to presentation is 4 years.[22] The most frequent locations are the retrobulbar muscle cone, especially the lateral aspect of the intraconal space.[31] However, a small minority (less than 10%) of these lesions are extraconal.[32] Cavernous hemangiomas rarely bleed[33] due to firmer texture from the surrounding support of rich fibrous tissue.[34] Orbital cavernous hemangiomas are typically solitary and unilateral, though multifocal and bilateral lesions have been reported.[35–38]

Imaging appearance

Cavernous hemangioma typically appears as a well-circumscribed intraconal mass.[39–42] Although most lesions are ovoid or round, larger lesions have lobulated margins. Larger lesions will distort surrounding structures, as opposed to lymphoma which molds around structures. CT shows homogeneous soft tissue density, and may show small calcifications or phleboliths.[39] MR shows isointense T1 signal, bright T2 signal, dark internal septations, and a dark circumferential rim that represents a fibrous pseudocapsule (Fig. 2).[22,34,43,44]

MR classically demonstrates nodular enhancement on early post-contrast images, and progressive accumulation of contrast on delayed post-contrast images.[31] The same findings are seen with multiphase CT, though concerns related to the increased radiation exposure of multiphase CT make this technique relatively less desirable. Small lesions often show early, uniform enhancement. MR angiography and CT angiography are generally not able to identify the

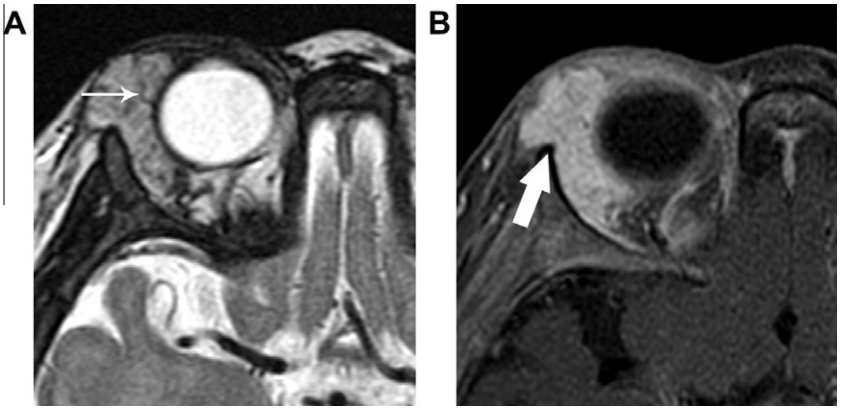

Figure 1. A 7 month-old girl with capillary (infantile) hemangioma. A. Axial T2 shows a well-defined, lobular, hyperintense mass with fine internal signal void (arrow) that likely represents an internal high-flow vessel. Septa in between lobules are slightly more linear. B. Axial fat-suppressed post contrast T1 shows intense, homogeneous enhancement typical of a proliferative phase lesion. The intact bony cortex at the zygoma is well demonstrated as a hypointense line (arrow).

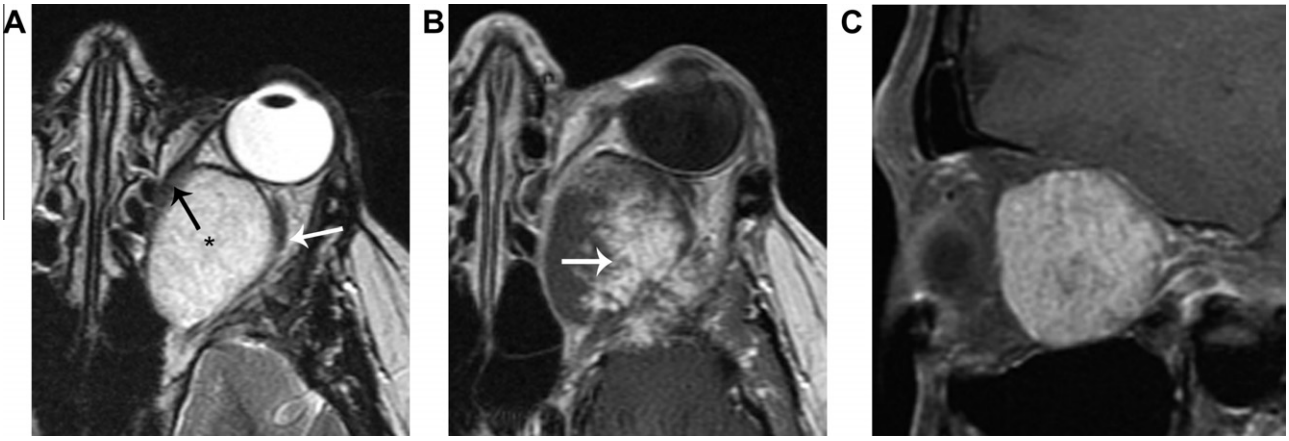

Figure 2. Cavernous hemangioma (solitary encapsulated venous-lymphatic malformation). A. Axial T2 shows an ovoid, homogeneous hyperintense mass (*) that distorts the medial rectus muscle (black arrow) and the optic nerve (white arrow). B. Axial T1 with contrast, obtained immediately after contrast injection, shows nodular enhancement. C. Para-sagittal oblique fat suppressed T1 with contrast, obtained 12 min after contrast injection, shows more uniform contrast enhancement. This slowly progressive nodular enhancement is typical of cavernous hemangioma, though also occasionally seen in schwannoma.

feeding vessels of a cavernous hemangioma, likely due to their small caliber.

Differential diagnosis

Venous varix, schwannoma, optic nerve sheath meningioma, and lymphoma.

Key imaging features

Intraconal location; very bright T2 signal with hypointense pseudocapsule; and an early nodular enhancement with progressive accumulation of contrast on later phase images.

Lymphangioma (venous lymphatic malformation)

Clinicopathologic features

'Lymphangiomas' are benign vascular malformations (venous lymphatic malformations), commonly affecting children and rarely involving the orbit. They are unencapsulated and composed of fibrous material including endothelial lacunae filled with blood or serious fluid.[45] Lymphangiomas tend to enlarge suddenly due to intralesional bleeding, but may also enlarge with upper respiratory infection.[46] Symptoms include: swelling, intraorbital hemorrhage, ocular proptosis, blepharoptosis and cellulitis. Ocular complications include: astigmatism, corneal exposure, hyperopia secondary to pressure on posterior globe, strabismus, glaucoma and compressive optic neuropathy.[47–49]

Imaging findings

Despite belonging to the same pathological category as 'cavernous hemangioma' (i.e. low flow vascular malformation without endothelial proliferation), lymphangioma has a different appearance and growth pattern. In keeping with their unencapsulated nature, lymphangiomas exhibit an infiltrative, trans-spatial growth pattern, often involving both the intraconal and extraconal compartments and pre- and post-septal compartments, violating fascial planes. Both microcysts and macrocysts may be identified.[50] CT may demonstrate phleboliths in the venous component of a lesion, and may demonstrate bony abnormalities.[46] Venous or solid components of the tumor are hyperdense compared to brain tissue on unenhanced CT scans.[50–52]

MR is accurate for delineating the anatomic location and vascular components, and fluid filled levels or menisci can be seen.[46] The mass is usually isointense to slightly hyperintense relative to normal brain tissue on T1 weighted imaging and very hyperintense relative to the brain on T2 weighted imaging[46], with internal septations (Fig. 3). T1 and T2 signal intensity vary depending on the presence and age of internal blood products. The venous component of a lesion will typically enhance, whereas the lymphatic component will only show fine enhancement of septations. No flow voids or enlarged feeder vessels are usually found, in keeping with the low flow nature of lymphangioma and differentiating it from high flow lesions, including high-flow vascular malformations and true neoplasms such as capillary hemangioma.[50,53,54]

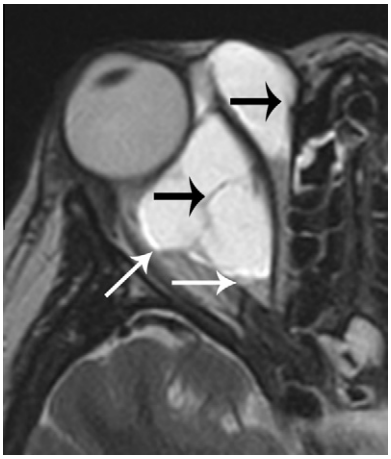

Figure 3. Lymphatic malformation (lymphangioma). Axial T2 shows a hyperintense, trans-spatial mass involving the intra- and extra-conal compartments. Hypointense septations (black arrows) are typical of this lesion. Layering blood products (white arrows) are variably present, and indicate recent intralesional bleeding.

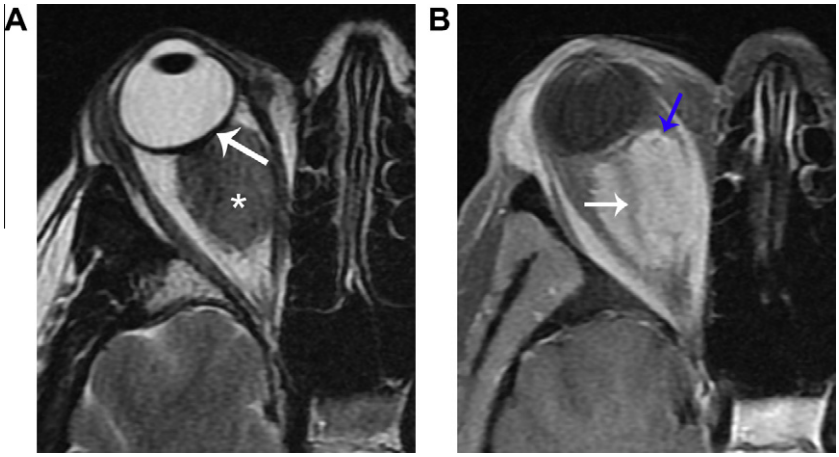

Figure 4. Optic nerve sheath meningioma. A. Axial T2 shows a homogeneous, hypointense mass (*) that mildly distorts the globe (arrow). B. Axial fat suppressed T1 with contrast shows homogeneous enhancement with a well-defined margin (blue arrow), and encasement of the optic nerve (white arrow). Globe distortion helps distinguish this lesion from lymphoma, as does the clinical history of slowly progressive, painless vision loss.

Differential diagnosis

Cavernous hemangioma, capillary hemangioma, dermoid, and rhabdomyosarcoma.

Key imaging features

Trans-spatial, markedly T2 bright non-enhancing mass with internal septations, with or without layering blood products and solidly enhancing components.

Benign neoplasms

Optic nerve sheath meningioma

Clinicopathologic features

The typical clinical presentation of optic nerve sheath meningioma is painless, gradual vision loss and proptosis in a woman between ages 30 and 50. Optic nerve sheath meningioma is typically unilateral but can be bilateral, particularly in the setting of type II neurofibromatosis. Primary meningioma arises from capillary cells of the arachnoid around the intraorbital or intracanalicular portions of the optic nerve. Secondary meningioma arises intracranially from the sphenoid ridge, tuberculum sellae, or olfactory groove and invades the optic canal and orbit by extension between the dura and arachnoid of the optic nerve.[55,56] Visual disturbance in the affected eye is common. While some patients only suffer transient visual loss lasting a few seconds, others experience visual loss in a particular field of gaze.[57,58] Optic neuropathy, proptosis and strabismus occur later.

Imaging findings

The key imaging finding of optic nerve sheath meningioma is a homogeneously enhancing mass that surrounds the optic nerve. CT may show calcification. MRI typically shows homogeneous, intermediate T1 and T2 signals. The optic nerve may be in the center of the lesion, or may be eccentrically positioned. In some cases, the optic nerve will show abnormal T2 hyperintense signal, which is presumably related to chronic venous insufficiency.

Optic nerve sheath meningioma may produce an expansile mass (Fig. 4). Alternatively, it may only form a thin sheet around the optic nerve, termed ''en plaque meningioma'', producing the classically described 'tram track' sign.[59] In these cases, fat-suppressed post-contrast T1-weighted images in the coronal plane are essential in making the diagnosis (Fig. 5). Any part of the nerve may be involved, and radiologic diagnosis can be challenging when only the intracanalicular portion of the nerve is affected. Fat suppression is helpful in these cases, but can also be degraded by blooming artifact around a well-pneumatized sphenoid sinus. For this reason, coronal post-contrast images without fat suppression should also be considered.

Optic nerve sheath meningioma is distinguished from optic glioma by the fact that the optic glioma expands the optic nerve. Orbital lymphoma can sometimes surround the optic nerve and simulate optic nerve sheath meningioma by imaging (Fig. 6). In such cases, lymphoma's tendency to mold around structures helps differentiate it from meningioma, which tends to distort structures. Lymphoma also typically shows less intense enhancement than meningioma. Meningioma frequently shows calcification on CT, whereas untreated lymphoma almost never calcifies. Perineuritic inflammatory disease can produce a similar appearance to en plaque meningioma, but is clinically distinguished by the presence of pain. Demyelinating optic neuritis is distinguished from en plaque meningioma by its typical homogeneous enhancement of the substance of the nerve, as opposed to the target-like enhancement of meningioma.

Differential diagnosis

Sarcoidosis, pseudotumors, lymphoma, and optic neuritis.

Key imaging features

Mass surrounding and constricting the optic nerve; calcification on CT; extension of tumor into the optic canal; ''tram track'' or ''target'' like enhancement.

Nerve sheath tumors

Clinicopathologic features

Nerve sheath tumors can be divided into schwannomas and neurofibromas, which are less common and typically associated with NF-1. Schwannomas constitute 1% of orbital tumors, typically occurring in young and middle-aged

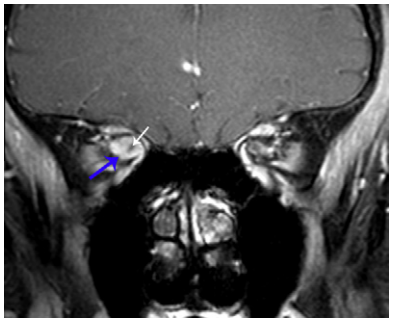

Figure 5. En plaque optic nerve sheath meningioma. Coronal fat suppressed T1 with contrast shows an enhancing mass (blue arrow) surrounding and constricting the optic nerve (white arrow). Fat suppressed post contrast coronal images are essential in identifying meningiomas with this growth pattern.

adults.[30,60] They typically arise from intraorbital branches of V1,[60] and produce symptoms related to local mass effect. Schwannomas are associated with NF-1 in 2–18% of patients.[61] Neurofibromas are more strongly associated with NF-1, and also produce symptoms related to mass effect.

Imaging findings

Schwannoma appears as a smooth, ovoid, orbital retrobulbar mass, found in the intra- or extra-conal space with the long axis in the anterior–posterior direction (Fig. 7).[39,62] CT shows isodensity or hypodensity compared to gray matter. MR shows isointense T1 signal, and T2 hyperintensity. Although some schwannomas may be cystic and non-enhancing,[63] most schwannomas enhance with contrast. Although schwannoma enhancement is typically more homogeneous than cavernous hemangioma, in some cases schwannoma can show the same type of early nodular enhancement with progressive fill-in that is commonly seen with cavernous hemangioma. The MR and CT appearance of schwannoma can overlap with optic nerve sheath meningioma. In challenging cases, one should look carefully for extension into the superior orbital fissure, which would favor schwannoma, or for extension into the optic canal, which would favor meningioma. Neurofibromas often have a similar appearance to schwannomas, though plexiform neurofibromas typically show a more infiltrative growth pattern (Fig. 8), and are frequently associated with other stigmata of NF-1.

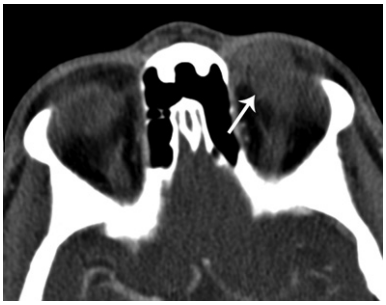

Figure 7. Schwannoma. Axial CT with contrast shows a hypodense, well-defined, extraconal mass with only weak enhancement. This appearance is nonspecific, and is often seen with schwannoma in addition to other benign and malignant masses.

Figure 8. Plexiform neurofibroma. Axial fat suppressed T2 shows a hyperintense mass in the left orbit, with extension through the superior orbital fissure (arrow) into the parasellar region.

Differential diagnosis

Cavernous hemangioma, meningioma, and lymphoma.

Key imaging features

Smooth, homogeneous spherical mass. Extension into superior orbital fissure. Enhancement is typically more

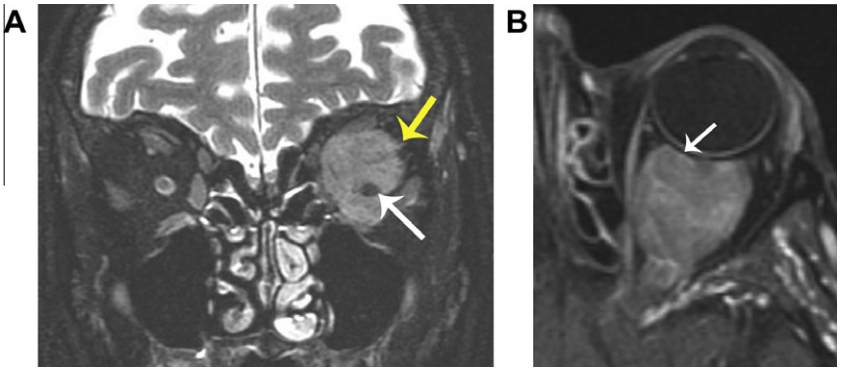

Figure 6. Lymphoma. A. Coronal fat suppressed T2 shows a homogeneous, somewhat hypointense mass that surrounds the optic nerve (white arrow). Although the mass is mostly well-defined, there is a slightly ill-defined lateral margin (yellow arrow). B. Axial fat suppressed T1 shows molding around the globe without globe distortion (arrow). Although optic nerve encasement is typical of meningioma, molding around the globe and poor margin definition are features that suggest lymphoma. Lymphoma also commonly shows slightly less intense enhancement than meningioma, as demonstrated in this case compared to Fig. 4.

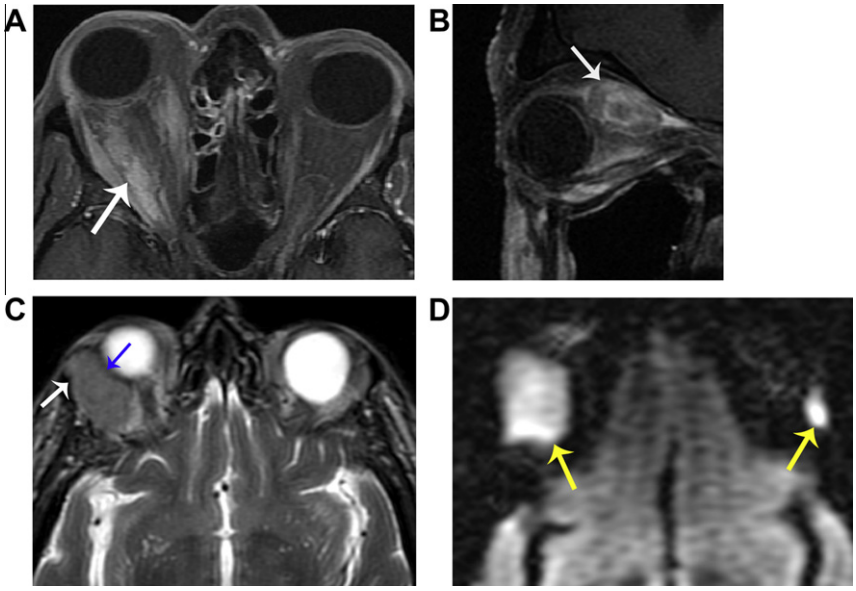

Figure 9. Lymphoma (multiple cases). A. Axial fat suppressed T1 with contrast shows ill-defined intraconal enhancement (arrow), representing infiltrative tumor. B. Parasagittal oblique T1 with contrast in a different patient shows an enhancing mass expanding the superior rectus muscle (arrow). C. Axial T2 in a third patient shows diffuse expansion of the right lacrimal gland, with slightly lobular contour. The mass respects the cortex of the zygoma (white arrow) and molds around the globe without distorting it (blue arrow). D. Axial DWI (same patient as 'C') shows very bright signal in both lacrimal glands (yellow arrows), reflecting involvement by hypercellular tumor. Left lacrimal gland disease is better detected with DWI than with conventional images, due to the relatively normal size of the gland and homogeneous appearance.

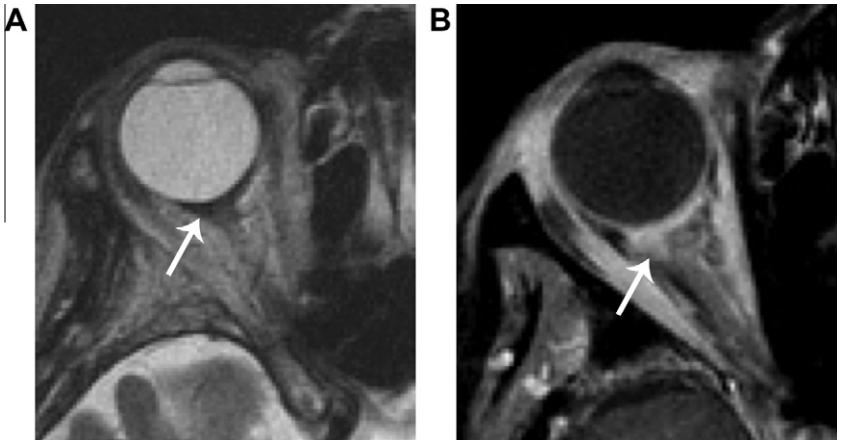

Figure 10. Breast cancer metastasis. A. Axial T2 shows a hypointense retrobulbar mass (arrow) that produces slight posterior tenting of the globe. B. Axial fat suppressed T1 with contrast shows ill-defined enhancement. Enophthalmos and a T2 dark mass are highly suggestive of breast cancer metastasis.

heterogeneous than lymphoma or meningioma, but less nodular than cavernous hemangioma.

Malignant neoplasms

Orbital lymphoid tumors (including malignant lymphoma)

Clinicopathologic features

Reactive lymphoid lesions overlap histologically with malignant lymphoma, and are sometimes grouped as 'orbital lymphoid lesions'.[64] The typical presentation is low-grade proptosis with minimal pain.[1] Lymphoid masses comprise 10–15% of all orbital tumors[65] and up to 55% of malignant orbital masses.[66] Malignant lymphoma of the orbit is typically B cell lymphoma of a non-Hodgkin type, arising from mucosa-associated lymphoid tissue of ocular adnexa (MALTOMA).[67] Systemic lymphoma may involve the orbit in 1.5–5% of patients.[68,69] Up to 75% of patients with orbital lymphoma may later develop systemic disease.[70] Suspicion of malignant lymphoma is increased in the presence of systemic disease, lacrimal duct or gland disease, and bilateral disease.[71]

Image appearance

Lymphoid tumors typically appear as homogeneous, lobulated masses on CT and MRI. They mold around normal structures without deforming them, and typically do not erode adjacent bone. They may be well defined, or infiltrative in appearance. CT shows density similar to skeletal muscle.

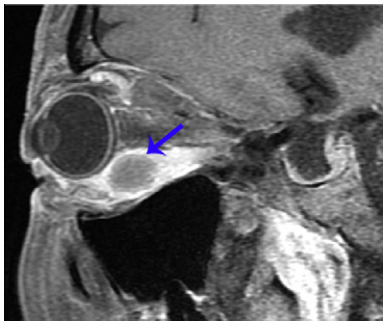

Figure 11. Carcinoid tumor metastasis. Parasagittal oblique fat suppressed T1 with contrast shows a peripherally enhancing mass centered in the distal portion of the inferior rectus muscle (arrow).

MRI demonstrates homogenous, intermediate T1 and T2 signals, and homogeneous contrast enhancement.[64,72,73]

Lymphomas most commonly involve the superolateral aspect of the orbit,[72] and bilateral disease is common.[1] When multiple sites of disease are present, the intraconal space is most affected (85%). Lymphoma can involve virtually any part of the orbit, including the lacrimal gland, extraocular muscles, lacrimal sac, periorbital fat, and retrobulbar fat (Fig. 9).

Lymphoma can be very difficult to distinguish from orbital inflammatory disease (''pseudotumor''). However, diffusion-weighted imaging (DWI) is an MRI technique that has recently been proven effective in distinguishing these entities. Lymphoma typically shows brighter DWI signal and lower apparent diffusion coefficient (ADC) than normal orbital structures, due to its hypercellular nature. Inflammatory lesions, on the other hand, tend to show intermediate DWI and ADC signals, similar to normal lacrimal gland.[27] Very low T2 signal (darker than normal white matter) should also suggest an inflammatory lesion.[5] DWI is also helpful for identifying lacrimal gland lymphoma.

Differential diagnosis

Orbital inflammatory syndrome, optic nerve sheath meningioma, and orbital metastasis.

Key imaging features (lymphoma)

Homogeneous intermediate T2 signal, lobulated margins with molding around normal structures, homogeneous enhancement, brighter DWI signal and lower ADC than surrounding normal orbital tissues.

Metastatic tumors of the orbit

Clinicopathologic features

In adults orbital metastases usually arise from carcinomatous origin, in children sarcomatous or neural embryonal tumors are more common.[74] The spread of tumor to the orbit and ocular adnexa is usually due to hematogenous spread of primary cancer, and is associated with a poor prognosis. Primary metastatic orbital tumors are estimated to account for 1–13% of all orbital tumors, and in cancer patients are prevalent from 2% to 4.7%.[75] Improved cancer therapy, improved diagnostic imaging and increased awareness in medical literature have allowed for better diagnosis of these tumors.

Metastatic lesions are found more in the anterior orbit than the posterior orbit.[76] The most frequent metastases to the orbit are from: breast, lung, prostate, melanoma, carcinoid, GI, renal cell, neuroblastomas and rhabdomyosarcomas. Rapidly progressive symptoms occur including: diplopia, proptosis, decreased vision, pain, ptosis, and palpable mass.[75]

Imaging findings

CT is usually performed for orbital imaging, although MR has superior soft tissue contrast. Tumor pattern can vary from diffusely infiltrative with obscured anatomical landmarks to a focal well-defined mass. Orbital metastases from breast cancer are often diffuse and irregular growing along the rectus muscles and fascial planes.[76] Scirrhous (fibrotic) breast cancers are unique in their ability to produce enophthalmos and ophthalmoplegia. In these cases, the metastatic lesion is typically very T2 dark, reflecting its fibrotic nature (Fig. 10). Metastases from carcinoid (Fig. 11), renal cell carcinoma and melanoma tend to be circumscribed. All orbital metastases show some degree of MR enhancement.[77] Metastases may involve any structure in the orbit, including the intraconal or extraconal space, globe, extraocular muscles and bone (Fig. 12).

Differential diagnosis

Lymphoma, infection, dysthyroid orbitopathy, orbital inflammatory disease, carotid cavernous fistula, and cavernous sinus thrombosis.

Key imaging findings

Imaging findings vary widely. Globe retraction is highly suspicious for scirrhous breast cancer metastasis.

Rhabdomyosarcoma

Clinicopathologic features

This is the most common soft tissue malignancy of childhood and most common primary orbital malignancy.[78,79] There is a bimodal distribution of affected ages, commonly occurring between 2 and 5 years[80] but is reported in all age groups.[81] The embryonal subtype occurs in childhood (mean age 8 years; male to female ratio 5:3); the pleomorphic subtype occurs in adults; the alveolar subtype occurs in young children and adults and is associated with a poor prognosis.[79]

Primary rhabdomyosarcoma can occur from the conjunctiva, iris, ciliary body, or extension of primary orbital rhabdomyosarcoma.[82] Secondary orbital rhabdomyosarcoma occurs

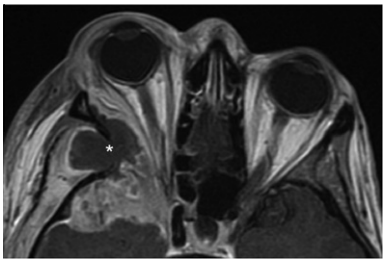

Figure 12. Colonic adenocarcinoma metastasis. Axial T1 with contrast shows a necrotic mass centered in the right sphenoid triangle (*), with enhancing tumor and surrounding inflammation along the margins extending into the middle cranial fossa and extraconal orbit.

Figure 13. A 26 year-old woman with rhabdomyosarcoma. CT shows an aggressive mass that deforms the globe and grossly destroys bone (arrow), invading the ethmoid sinus through the lamina papyracea.

from direct extension to orbits from the paranasal sinus, pterygopalatine fossa, infratemporal fossa or nasopharynx. Orbital metastases can also occur from other head and neck rhabdomyosarcomas and carries a poor prognosis. The orbital location varies: extraconal (37%), intraconal (17%), both (47%). The upper outer quadrant is involved in 67%. Presenting complaints include: unilateral proptosis (80–100%), globe displacement (80%), ptosis (30–50%), conjunctival and eyelid swelling (60%), palpable mass (25%), and pain (10%).[83,84]

Imaging findings

CT shows moderately well defined to ill-defined margins, irregular shape, and mild-moderate contrast enhancement. Adjacent bony destruction occurs in 40% (Fig. 13). Globe distortion[85] and extension to the paranasal sinuses[82,86] may also be seen. Regional lymph nodes are involved later in the disease course. Calcification is rare in untreated tumors.

MR typically shows bright T2 signal, distinguishing rhabdomyosarcoma from other tumors such as chloroma (granulocytic sarcoma), lymphoma and metastatic neuroblastoma (Fig. 14). MR may also better delineate the true extent of disease if surgical resection is planned.[87] On occasion, a pyogenic abscess may have a subacute presentation that mimics a necrotic rhabdomyosarcoma clinically and by imaging.[88] In such cases, MRI with DWI is critical in distinguishing these entities, through demonstration of restricted diffusion of pus in an abscess cavity,[89] as opposed to elevated diffusion in the necrotic portion of a tumor.[90]

Differential diagnosis

Leukemic metastatic deposits; Langerhans cell histiocytosis; aggressive fibromatosis; ruptured dermoid cyst; subperiosteal hematoma; plexiform neurofibromatosis, capillary hemangioma.

Key imaging features

CT: variable definition, bony destruction; MR: bright T2 signal.

Optic nerve glioma

Clinicopathologic features

Optic nerve glioma comprises 1.5–3.0% of orbital tumors, 0.6–7.0% of all intracranial tumors, 1.7–7.0% of gliomas, and 2–5% of gliomas in the pediatric age group.[91,92] The peak incidence is in 2–8 year old but can occur at any age and has been reported at up to 79 years of age.[93,94] Females are more affected than males. There is a high association (12–37%) with type I neurofibromatosis type 1[95], which frequently shows bilateral lesions. Notably, optic gliomas associated with NF-1 typically have more indolent behavior than isolated optic nerve gliomas. Symptoms include: proptosis, decreased visual acuity,[96] nystagmus, strabismus, central/paracentral field defects, dyschromatopsia, and afferent pupillary defect.[92] Disk edema and atrophy may be evident by 8 weeks. The tumors are slow growing with periods of growth and dormancy,[97,98] some may regress completely.[99,100] In an analysis of affected orbital locations, 48% involved the orbital optic nerve, 24% the orbital and intracranial optic nerve, 10% intracranial optic nerve and chiasm, and just chiasm in up to 5%.[101] Surgery is typically reserved for cases where there is significant mass effect.

Imaging findings

MR is optimal for imaging optic nerve glioma.[102] The classic finding of optic nerve glioma is sharply circumscribed fusiform thickening and tortuosity of the optic nerve. Optic gliomas are typically T2 hyperintense, and usually show some

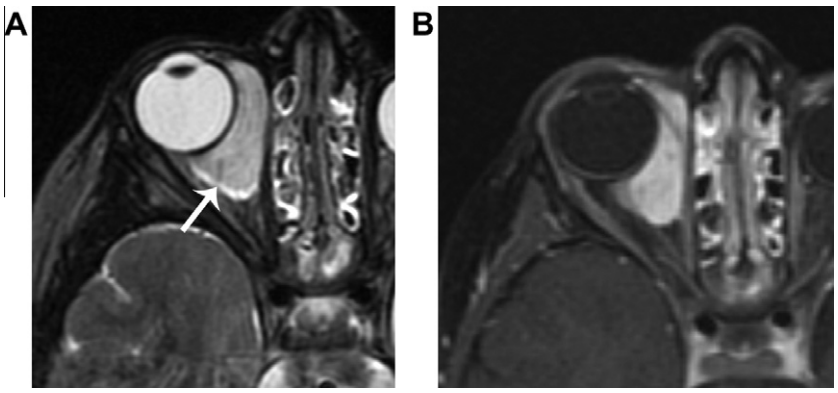

Figure 14. A 3 year-old boy with embryonal rhabdomyosarcoma. A. Axial T2 shows a well-defined, hyperintense mass involving the retrobulbar and extraconal soft tissues, without destruction of the bone or distortion of adjacent structures. B. Axial fat-suppressed T1 with contrast shows intense, homogeneous enhancement. This mass has certain features that are common to capillary hemangioma. However, continued growth of the mass after the first year of life, absence of flow voids, and absence of discrete lobules with T2 hypointense septations, are features that suggest an alternative diagnosis.

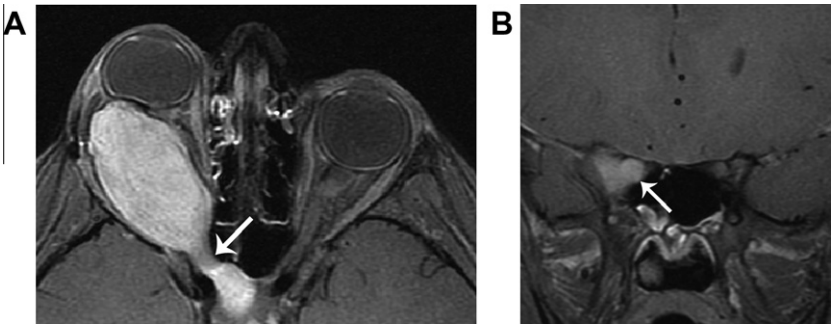

Figure 15. Optic glioma. A. Axial fat-suppressed T1 with contrast shows a solidly enhancing dumbbell-shaped mass extending through the right optic canal (arrow). B. Coronal fat-suppressed T1 with contrast shows diffuse enhancement of the substance of the right optic nerve (arrow), a finding that confirms optic glioma rather than optic nerve sheath meningioma. Meningioma forms an enhancing mass that surrounds and constricts the optic nerve.

enhancement, though a wide range of signal intensities and enhancement patterns may be encountered.[103] Diffuse involvement of the substance of the nerve differentiates optic nerve glioma from optic nerve sheath meningioma, which surrounds the optic nerve. Any part of the optic nerve may be involved, from the globe to the optic chiasm. Peripheral enhancement of chiasmatic gliomas represents extraneural growth of tumor into the subarachnoid space, mixed with gliomatous tissue and non enhancing central tumor. Optic nerve gliomas that extend to the chiasm through the optic canal form a dumbbell shape (Fig. 15).

Differential diagnosis

Optic nerve sheath meningioma and medulloepithelioma.

Key imaging features

Diffuse enlargement of the substance of the optic nerve, with thickening and tortuosity.

Conclusion

A wide variety of lesions may be encountered in the orbit. Knowledge of the most common lesions, their typical clinical presentation, typical imaging appearance, and key features that distinguish from similar lesions should allow the reader to make the best use of imaging.

References

1. Kapur R, Sepahdari AR, Mafee MF, et al. MR imaging of orbital inflammatory syndrome, orbital cellulitis, and orbital lymphoid lesions: the role of diffusion-weighted imaging. *AJNR Am J Neuroradiol* 2009;**30**(1):64–70.
2. Uehara F, Ohba N. Diagnostic imaging in patients with orbital cellulitis and inflammatory pseudotumor. *Int Ophthalmol Clin* 2002;**42**(1):133–42.
3. Som P, Curtin H. Head and neck imaging; 2011.
4. Yuen SJ, Rubin PA. Idiopathic orbital inflammation: distribution, clinical features, and treatment outcome. *Archiv Ophthalmol* 2003;**121**(4):491–9.
5. Cytryn AS, Putterman AM, Schneck GL, Beckman E, Valvassori GE. Predictability of magnetic resonance imaging in differentiation of orbital lymphoma from orbital inflammatory syndrome. *Ophthalmic Plast Reconstr Surg* 1997;**13**(2):129–34.
6. Yan J, Wu Z, Li Y. The differentiation of idiopathic inflammatory pseudotumor from lymphoid tumors of orbit: analysis of 319 cases. *Orbit* 2004;**23**(4):245–54.
7. Shields JA, Shields CL, Scartozzi R. Survey of 1264 patients with orbital tumors and simulating lesions: The 2002 Montgomery Lecture. Part 1. *Ophthalmology* 2004;**111**(5):997–1008.
8. Smoker WR, Gentry LR, Yee NK, Reede DL, Nerad JA. Vascular lesions of the orbit: more than meets the eye. *Radiograph: A Rev Publ Radiol Soc North America, Inc.* 2008;**28**(1):185–204 quiz 325.
9. Bilaniuk LT. Vascular lesions of the orbit in children. *Neuroimag Clin North America* 2005;**15**(1):107–20.
10. Goawalla A, Mansell N, Pearson A. Septic cavernous sinus thrombosis with bilateral secondary orbital infection. *Orbit* 2007;**26**(2):113–6.
11. Patel R, Mukherjee B. Mesenchymal chondrosarcoma of the orbit. *Orbit* 2012;**31**(2):126–8.
12. Yang BT, Wang YZ, Wang XY, Wang ZC. Mesenchymal chondrosarcoma of the orbit: CT and MRI findings. *Clin Radiol* 2012;**67**(4):346–51.
13. Kousoubris PD, Rosman DA. Radiologic evaluation of lacrimal and orbital disease. *Otolaryng Clin North America* 2006;**39**(5):865–93 vi.
14. Mafee MF, Edward DP, Koeller KK, Dorodi S. Lacrimal gland tumors and simulating lesions. Clinicopathologic and MR imaging features. *Radiol Clin North America* 1999;**37**(1):219–39 xii.
15. Vajaranant TS, Mafee MF, Kapur R, Rapoport M, Edward DP. Medulloepithelioma of the ciliary body and optic nerve: clinicopathologic, CT, and MR imaging features. *Neuroimag Clin North America* 2005;**15**(1):69–83.
16. Eijpe AA, Koornneef L, Bras J, Verbeeten Jr B, Peeters FL, Zonneveld FW. Dermolipoma: characteristic CT appearance. *Doc ophthalmol. Adv Ophthalmol* 1990;**74**(4):321–8.
17. Kim E, Kim HJ, Kim YD, Woo KI, Lee H, Kim ST. Subconjunctival fat prolapse and dermolipoma of the orbit: differentiation on CT and MR imaging. *AJNR Am J Neuroradiol* 2011;**32**(3):465–7.
18. Pham NS, Dublin AB, Strong EB. Dermoid cyst of the orbit and frontal sinus: a case report. *Skull Base: Off J North American Skull Base Soc.....et al.* 2010;**20**(4):275–8.
19. Yeola M, Joharapurkar SR, Bhole AM, Chawla M, Chopra S, Paliwal A. Orbital floor dermoid: an unusual presentation. *Indian J Ophthalmol* 2009;**57**(1):51–2.
20. Jung WS, Ahn KJ, Park MR, et al. The radiological spectrum of orbital pathologies that involve the lacrimal gland and the lacrimal fossa. *Korean J Radiol: Off J Korean Radiol Soc* 2007;**8**(4):336–42.
21. Mulliken JB, Glowacki J. Hemangiomas and vascular malformations in infants and children: a classification based on endothelial characteristics. *Plast Reconstr Surg* 1982;**69**(3):412–22.
22. Bilaniuk LT. Orbital vascular lesions. Role of imaging. *Radiol Clin North America* 1999;**37**(1):169–83 xi.
23. Haik BG, Karcioglu ZA, Gordon RA, Pechous BP. Capillary hemangioma (infantile periocular hemangioma). *Surv Ophthalmol* 1994;**38**(5):399–426.
24. Dubois J, Garel L. Imaging and therapeutic approach of hemangiomas and vascular malformations in the pediatric age group. *Pediat Radiol* 1999;**29**(12):879–93.
25. Burrows PE, Laor T, Paltiel H, Robertson RL. Diagnostic imaging in the evaluation of vascular birthmarks. *Dermatol Clin* 1998;**16**(3):455–88.
26. Haik BG, Jakobiec FA, Ellsworth RM, Jones IS. Capillary hemangioma of the lids and orbit: an analysis of the clinical features and therapeutic results in 101 cases. *Ophthalmology* 1979;**86**(5):760–92.
27. Sepahdari AR, Aakalu VK, Setabutr P, Shiehmorteza M, Naheedy JH, Mafee MF. Indeterminate orbital masses: restricted diffusion at MR

imaging with echo-planar diffusion-weighted imaging predicts malignancy. *Radiology* 2010;**256**(2):554–64.
28. Politi LS, Forghani R, Godi C, et al. Ocular adnexal lymphoma: diffusion-weighted mr imaging for differential diagnosis and therapeutic monitoring. *Radiology* 2010;**256**(2):565–74.
29. Razek AA, Elkhamary S, Mousa A. Differentiation between benign and malignant orbital tumors at 3-T diffusion MR-imaging. *Neuroradiology* 2011;**53**(7):517–22.
30. Shields JA, Bakewell B, Augsburger JJ, Flanagan JC. Classification and incidence of space-occupying lesions of the orbit. A survey of 645 biopsies. *Archiv Ophthalmol* 1984;**102**(11):1606–11.
31. Ansari SA, Mafee MF. Orbital cavernous hemangioma: role of imaging. *Neuroimag Clin North America* 2005;**15**(1):137–58.
32. Harris GJ, Jakobiec FA. Cavernous hemangioma of the orbit. *J Neurosurg* 1979;**51**(2):219–28.
33. Zenobii M, Galzio RJ, Lucantoni D, Caffagni E, Magliani V. Spontaneous intraorbital hemorrhage caused by cavernous angioma of the orbit. *J Neurosurg Sci* 1984;**28**(1):37–40.
34. Thorn-Kany M, Arrue P, Delisle MB, Lacroix F, Lagarrigue J, Manelfe C. Cavernous hemangiomas of the orbit: MR imaging. *J Neuroradiol. J Neuroradiol* 1999;**26**(2):79–86.
35. Ruchman MC, Flanagan J. Cavernous hemangiomas of the orbit. *Ophthalmology* 1983;**90**(11):1328–36.
36. Wolin MJ, Holds JB, Anderson RL, Mamalis N. Multiple orbital tumors were cavernous hemangiomas. *Ann Ophthalmol* 1990;**22**(11):426–8.
37. Sullivan TJ, Aylward GW, Wright JE, Moseley IF, Garner A. Bilateral multiple cavernous haemangiomas of the orbit. *The Brit J Ophthalmol* 1992;**76**(10):627–9.
38. Shields JA, Hogan RN, Shields CL, Eagle Jr RC, Kennedy RH, Singh AD. Bilateral cavernous haemangiomas of the orbit. *The Brit J Ophthalmol* 2000;**84**(8):928.
39. Mafee MF, Putterman A, Valvassori GE, Campos M, Capek V. Orbital space-occupying lesions: role of computed tomography and magnetic resonance imaging. An analysis of 145 cases. *Radiol Clin North America* 1987;**25**(3):529–59.
40. Gyldensted C, Lester J, Fledelius H. Computed tomography of orbital lesions. A radiological study of 144 cases. *Neuroradiology* 1977;**13**(3):141–50.
41. Savoiardo M, Strada L, Passerini A. Cavernous hemangiomas of the orbit: value of CT, angiography, and phlebography. *AJNR Am J Neuroradiol* 1983;**4**(3):741–4.
42. Forbes GS, Sheedy 2nd PF, Waller RR. Orbital tumors evaluated by computed tomography. *Radiology* 1980;**136**(1):101–11.
43. Bilaniuk LT, Rapoport RJ. Magnetic resonance imaging of the orbit. *Top Magn Reson Imag: TMRI* 1994;**6**(3):167–81.
44. Fries PD, Char DH, Norman D. MR imaging of orbital cavernous hemangioma. *J Comput Assist Tomogr* 1987;**11**(3):418–21.
45. Lemke AJ, Kazi I, Felix R. Magnetic resonance imaging of orbital tumors. *Eur Radiol* 2006;**16**(10):2207–19.
46. Chung EM, Smirniotopoulos JG, Specht CS, Schroeder JW, Cube R. From the archives of the AFIP: Pediatric orbit tumors and tumorlike lesions: nonosseous lesions of the extraocular orbit. *Radiograph: A Rev Publ Radiol Soc North America, Inc.* 2007;**27**(6):1777–99.
47. Greene AK, Burrows PE, Smith L, Mulliken JB. Periorbital lymphatic malformation: clinical course and management in 42 patients. *Plast Reconstr Surg* 2005;**115**(1):22–30.
48. Coll GE, Goldberg RA, Krauss H, Bateman BJ. Concomitant lymphangioma and arteriovenous malformation of the orbit. *Am J Ophthalmol* 1991;**112**(2):200–5.
49. Eiferman RA, Gushard RH. Chocolate cysts of the orbit. *Ann Ophthalmol* 1986;**18**(4):156–7.
50. Bisdorff A, Mulliken JB, Carrico J, Robertson RL, Burrows PE. Intracranial vascular anomalies in patients with periorbital lymphatic and lymphaticovenous malformations. *AJNR Am J Neuroradiol* 2007;**28**(2):335–41.
51. Baker LL, Dillon WP, Hieshima GB, Dowd CF, Frieden IJ. Hemangiomas and vascular malformations of the head and neck: MR characterization. *AJNR Am J Neuroradiol* 1993;**14**(2):307–14.
52. Wright JE, Sullivan TJ, Garner A, Wulc AE, Moseley IF. Orbital venous anomalies. *Ophthalmology* 1997;**104**(6):905–13.
53. Forbes G. Vascular lesions in the orbit. *Neuroimag Clin North America* 1996;**6**(1):113–22 vii.
54. Castillo M, Mukherji SK, Wagle NS. Imaging of the pediatric orbit. *Neuroimag Clin North America* 2000;**10**(1):95–116 viii.
55. Miller NR. Primary tumours of the optic nerve and its sheath. *Eye (Lond)* 2004;**18**(11):1026–37.
56. Dutton JJ. Optic nerve gliomas and meningiomas. *Neurol Clin* 1991;**9**(1):163–77.
57. Bradbury PG, Levy IS, McDonald WI. Transient uniocular visual loss on deviation of the eye in association with intraorbital tumours. *J Neurol, Neurosurg, Psychiatr* 1987;**50**(5):615–9.
58. Oohira A, Kubo R. Ocular blood flow defect in gaze-evoked amaurosis. *Nippon Ganka Gakkai Zasshi* 1999;**103**(1):56–60.
59. Mafee MF, Goodwin J, Dorodi S. Optic nerve sheath meningiomas. Role of MR imaging. *Radiol Clin North America* 1999;**37**(1):37–58 ix.
60. Albert D. *Principles and practice of ophthalmology*. 2nd ed. Philadelphia: WB Saunders; 2000.
61. Gunduz K, Shields CL, Gunalp I, Erden E, Shields JA. Orbital schwannoma: correlation of magnetic resonance imaging and pathologic findings. *Graefe's Archiv Clin Exp Ophthalmol = Albrecht von Graefes Archiv klin exp Ophthalmol* 2003;**241**(7):593–7.
62. Dervin JE, Beaconsfield M, Wright JE, Moseley IF. CT findings in orbital tumours of nerve sheath origin. *Clin Radiol* 1989;**40**(5):475–9.
63. Lam DS, Ng JS, To KF, Abdulah V, Liew CT, Tso MO. Cystic schwannoma of the orbit. *Eye (Lond)* 1997;**11**(Pt 6):798–800.
64. Westacott S, Garner A, Moseley IF, Wright JE. Orbital lymphoma versus reactive lymphoid hyperplasia: an analysis of the use of computed tomography in differential diagnosis. *The Brit J Ophthalmol* 1991;**75**(12):722–5.
65. Peyster RG, Shapiro MD, Haik BG. Orbital metastasis: role of magnetic resonance imaging and computed tomography. *Radiol Clin North America* 1987;**25**(3):647–62.
66. Margo CE, Mulla ZD. Malignant tumors of the orbit. Analysis of the florida cancer registry. *Ophthalmology* 1998;**105**(1):185–90.
67. Valvassori GE, Sabnis SS, Mafee RF, Brown MS, Putterman A. Imaging of orbital lymphoproliferative disorders. *Radiol Clin North America* 1999;**37**(1):135–50 x–xi.
68. Rosenberg SA, Diamond HD, Jaslowitz B, Craver LF. Lymphosarcoma: a review of 1269 cases. *Medicine* 1961;**40**:31–84.
69. Bairey O, Kremer I, Rakowsky E, Hadar H, Shaklai M. Orbital and adnexal involvement in systemic non-Hodgkin's lymphoma. *Cancer* 1994;**73**(9):2395–9.
70. Flanders AE, Espinosa GA, Markiewicz DA, Howell DD. Orbital lymphoma. Role of CT and MRI. *Radiol Clin North America* 1987;**25**(3):601–13.
71. Akansel G, Hendrix L, Erickson BA, et al. MRI patterns in orbital malignant lymphoma and atypical lymphocytic infiltrates. *Eur J Radiol* 2005;**53**(2):175–81.
72. Hosten N, Schorner W, Zwicker C, et al. Lymphocytic infiltrations of the orbit in MRT and CT. Lymphoma, pseudolymphoma and inflammatory pseudotumor. *RoFo: Fortschritte auf dem Gebiete der Rontgenstrahlen und der Nuklearmedizin* 1991;**155**(5):445–51.
73. Issing PR, Ruh S, Kloss A, Kuske M, Lenarz T. Diagnosis and therapy of lymphoid tumors of the orbits. *Hno* 1997;**45**(7):545–50.
74. Garrity JA. Metastatic carcinomas*Henderson's orbital tumors*. New York: Raven Press; 2007. p. 313–26.
75. Ahmad SM, Esmaeli B. Metastatic tumors of the orbit and ocular adnexa. *Curr Opin Ophthalmol* 2007;**18**(5):405–13.
76. Shields JA, Shields CL, Brotman HK, Carvalho C, Perez N, Eagle Jr RC. Cancer metastatic to the orbit: the 2000 Robert M. Curts lecture. *Ophthal Plast Reconstr Surg* 2001;**17**(5):346–54.
77. DePotter PDC, Shields JA. *MRI of the eye and orbit*. Philadelphia: JB Lippincott Co.; 1995, pp. 237–43.
78. MacArthur CJ, McGill TJ, Healy GB. Pediatric head and neck rhabdomyosarcoma. *Clin Pediatr* 1992;**31**(2):66–70.
79. Volpe NJ, Jakobiec FA. Pediatric orbital tumors. *Int Ophthalmol Clin* 1992;**32**(1):201–21.
80. Walton RC, Ellis Jr GS, Haik BG. Rhabdomyosarcoma presumed metastatic to the orbit. *Ophthalmology* 1996;**103**(9):1512–6.
81. Shields JA, Shields CL. Rhabdomyosarcoma of the orbit. *Int Ophthalmol Clin* 1993;**33**(3):203–10.
82. Shields JA, Shields CL. Rhabdomyosarcoma: review for the ophthalmologist. *Surv Ophthalmol* 2003;**48**(1):39–57.
83. Jones IS, Reese AB, Kraut J. Orbital rhabdomyosarcoma. An analysis of 62 cases. *Am J Ophthalmol* 1966;**61**(4):721–36.
84. Jones IS, Reese AB, Krout J. Orbital rhabdomyosarcoma: an analysis of sixty-two cases. *Trans Am Ophthalmol Soc* 1965;**63**:223–55.
85. Sohaib SA, Moseley I, Wright JE. Orbital rhabdomyosarcoma – the radiological characteristics. *Clin Radiol* 1998;**53**(5):357–62.

86. Folpe AL, McKenney JK, Bridge JA, Weiss SW. Sclerosing rhabdomyosarcoma in adults: report of four cases of a hyalinizing, matrix-rich variant of rhabdomyosarcoma that may be confused with osteosarcoma, chondrosarcoma, or angiosarcoma. *Am J Surg Pathol* 2002;**26**(9):1175–83.
87. Mafee MF, Pai E, Philip B. Rhabdomyosarcoma of the orbit. Evaluation with MR imaging and CT. *Radiol Clin North America* 1998;**36**(6):1215–27 xii.
88. Cota N, Chandna A, Abernethy LJ. Orbital abscess masquerading as a rhabdomyosarcoma. *J AAPOS: The Off Publ Am Assoc Pediatr Ophthalmol Strab/Am Assoc Pediatr Ophthalmol Strab* 2000;**4**(5):318–20.
89. Sepahdari AR, Aakalu VK, Kapur R, et al. MRI of orbital cellulitis and orbital abscess: the role of diffusion-weighted imaging. *AJR Am J Roentgenol* 2009;**193**(3):W244–50.
90. Koc O, Paksoy Y, Erayman I, Kivrak AS, Arbag H. Role of diffusion weighted MR in the discrimination diagnosis of the cystic and/or necrotic head and neck lesions. *Eur J Radiol* 2007;**62**(2):205–13.
91. Dutton JJ. Gliomas of the anterior visual pathway. *Surv Ophthalmol* 1994;**38**(5):427–52.
92. Thompson CR, Lessell S. Anterior visual pathway gliomas. *Int Ophthalmol Clin* 1997;**37**(4):261–79.
93. Lertchavanakul A, Baimai C, Siwanuwatn R, Nuchprayoon I, Phudhichareonrat S. Optic nerve glioma in infancy: a case report of the youngest patient in Thailand. *J Med Assoc Thailand = Chotmaihet Thangphaet* 2001;**84**(Suppl 1):S137–41.
94. Wulc AE, Bergin DJ, Barnes D, Scaravilli F, Wright JE, McDonald WI. Orbital optic nerve glioma in adult life. *Archiv Ophthalmol* 1989;**107**(7):1013–6.
95. Spencer W. Optic nerve. In: Spencer WH, editor. *Ophthalmic pathology*, vol. 3. Philadelphia7: WB Saunders; 1996. p. 513–622.
96. Cirak B. Optic nerve glioma. *J Neurosurg* 2003;**99**(2 Suppl):246 Author reply 246.
97. Borit A, Richardson Jr EP. The biological and clinical behaviour of pilocytic astrocytomas of the optic pathways. *Brain: A J Neurol* 1982;**105**(Pt 1):161–87.
98. Thiagalingam S, Flaherty M, Billson F, North K. Neurofibromatosis type 1 and optic pathway gliomas: follow-up of 54 patients. *Ophthalmology* 2004;**111**(3):568–77.
99. Parazzini C, Triulzi F, Bianchini E, et al. Spontaneous involution of optic pathway lesions in neurofibromatosis type 1: serial contrast MR evaluation. *AJNR Am J Neuroradiol* 1995;**16**(8):1711–8.
100. Parsa CF, Hoyt CS, Lesser RL, et al. Spontaneous regression of optic gliomas: thirteen cases documented by serial neuroimaging. *Archiv Ophthalmol* 2001;**119**(4):516–29.
101. Davis R. Juvenile pilocytic astrocytoma of the optic nerve: clinico-pathologic study of sixty three cases. In: Jakobiec FA, editor. *Ocular and adnexal tumors*. Birmingham7 Yanoff Aesculapius; 1978. p. 685–707.
102. Holman RE, Grimson BS, Drayer BP, Buckley EG, Brennan MW. Magnetic resonance imaging of optic gliomas. *Am J Ophthalmol* 1985;**100**(4):596–601.
103. Weber AL, Klufas R, Pless M. Imaging evaluation of the optic nerve and visual pathway including cranial nerves affecting the visual pathway. *Neuroimag Clin North America* 1996;**6**(1):143–77.